



Volumetric, Optical and Spectroscopic Properties of Binary Mixtures of Glycerol with Butanediol Isomers

Yasmine Chabouni¹ · Ariel Hernández² · Fouzia Amireche¹

Received: 26 August 2023 / Accepted: 1 October 2023 / Published online: 20 October 2023

© The Author(s), under exclusive licence to Springer Science+Business Media, LLC, part of Springer Nature 2023

Abstract

The presented work is a part of a research study on the volumetric, optical, and spectroscopic properties of binary mixtures containing glycerol with the four isomers of butanediol, namely: 1,2-butanediol or 1,3-butanediol or 1,4-butanediol or 2,3-butanediol. The density and refractive index measurements of pure components and their binary mixtures were carried out at atmospheric pressure and in a temperature range from 293.15 K to 318.15 K. The experimental data were then used to calculate for each system the following derived properties as a function of temperature and glycerol concentration: excess molar volumes, V^E , partial molar volumes, \bar{V}_i , apparent molar volumes, $V_{\phi i}$, partial molar volumes at infinite dilution, \bar{V}_i^∞ , excess partial molar volume at infinite dilution, $\overline{V}_i^{E\infty}$, isobaric thermal expansions, α , excess thermal expansions, α^E , and refractive index deviations, Δn_D . Infrared spectroscopy analysis was also performed at atmospheric temperature and pressure. The experimental data obtained were fitted using the polynomial equation of Redlich-Kister. Excess molar volumes V^E for all the studied systems are negative over the entire composition range and at all the considered temperatures with deviations from ideality increasing with increasing temperature. The calculated molar excess properties were well correlated by the empirical Redlich-Kister polynomial. All measured and calculated properties reveal a significant influence of molecule structure, including the size, shape and position of the component hydroxyl groups. As intended, the infrared spectra of these binary mixtures display a high potential for hydrogen bonding. PC-SAFT EoS was successfully used to adjust the vapor pressure and liquid density of pure fluids, and was used predictively to correctly obtain the density of the mixture. Laplace's rule was used to predict the refractive index of mixtures.

Keywords Butanediol isomers · Density · Glycerol · PC-SAFT EoS · Refractive index · Spectroscopic properties

Extended author information available on the last page of the article

1 Introduction

The massive production of biodiesel to cover the growing need for energy while simultaneously reducing the impact of gas emissions generates relatively large volumes of the main by-product, glycerol [1, 2]. The challenge, therefore, is to provide the appropriate added value, making the entire biodiesel production chain more sustainable. For this purpose, glycerol has been the focus of much attention in recent years, and has a role in virtually every industry, either as a raw material or as an intermediate in reactions. Glycerol is often used as a lubricant, humectant and emulsifier in the cosmetics and pharmaceutical industries, as an additive and a stabilizer in the food industry, as a single user in alkyl resin and as a plasticizer in cellophane manufacture. One of glycerol's oldest industrial uses is as a cryoprotective agent. It is also in great demand as a solvent in the chemical industry, such as its conversion into ethanol, 1,2-propanediol and 1,3-propanediol, 2,3-butanediol, n-butanol, dihydroxyacetone, succinic acid, polyols and numerous other compounds [3, 4]. All these technical applications require knowledge of the thermophysical properties of pure substances and mixtures. In thermodynamic engineering, these properties often complement phase equilibrium values. From a fundamental point of view, in addition to structural effects, they can also account for the energetic aspects governing liquid mixtures, i.e. the various molecular interactions. In addition, they are used as technical data in the design and optimization of technological processes, as well as in the resolution of numerous engineering problems [5–7]. These properties can also be exploited to develop new predictive models or improve existing ones. The purpose of the current paper is to provide reliable data on the density and refractive index of four binary mixtures including glycerol with 1,2-butanediol, 1,3-butanediol, 1,4-butanediol, and 2,3-butanediol, all of which are widely used in industry. Based on these experimental data, we calculated the following derived thermodynamic properties: excess molar volume V^E , partial molar volume \bar{V}_i , apparent molar volume V_θ , thermal expansion coefficient α , excess thermal expansion coefficient α^E , excess partial molar volume at infinite dilution \bar{V}_i^∞ , excess partial molar volume at infinite dilution $\bar{V}_i^{E\infty}$, refractive index variation Δn_D . Excess properties were correlated using the empirical Redlich-Kister equation for all binary mixtures. Detailed analysis of these excess properties revealed the likelihood of molecular interactions in the various mixtures. To this end, an infrared mode study (FT-IR) of all the binary mixtures was carried out. The results suggest the presence of intermolecular hydrogen-bonding interactions between the various hydroxyl groups in the alcohol-rich mixtures, through displacement and broadening of the (–OH) vibrational band.

Finally, in this study, PC-SAFT EoS was used to calculate the density for pure fluids and binary mixtures. We have used Laplace's mixing rule + PC-SAFT EoS to predict the refractive index.

2 Experimental Section

2.1 Materials

The samples were supplied by Merck and were of analytical grade, the details about their purity are given in Table 1. The purity of the chemicals was confirmed using perkin elmer gas chromatography clarus 500 with TCD detector (Oven temperature 100–190 at $4\text{ }^{\circ}\text{C min}^{-1}$; injector temperature: $220\text{ }^{\circ}\text{C}$; detector temperature: $230\text{ }^{\circ}\text{C}$) and an Agilent J & W SE-30 column of 30 m length, 0.53 mm inner diameter, and $0.5\text{ }\mu\text{m}$ thickness is used in the separation. The chromatogram for individual species showed a single peak signifying no impurity and hence they were used directly without any purification. Enantiomeric composition analyses of the 2,3-butanediol (mixture of meso-D- and L form) were performed using the established GC-FID analysis method [8]: GC-FID, column temperature: $95\text{ }^{\circ}\text{C}$ – $130\text{ }^{\circ}\text{C}$ ($1.0\text{ }^{\circ}\text{C min}^{-1}$), injector temperature of $145\text{ }^{\circ}\text{C}$. Retention times (min): (+)-2 S,3 S-butanediol, 7.72; (–)-2R,3R-butanediol, 8.06; meso-butanediol, 8.53. All the analysis were repeated three times and the results are arithmetic mean values. All liquids were stored over molecular sieves (5 \AA) in dark-colored bottles to avoid water absorption. The purity of the chemicals was also checked by comparing their densities ρ , and refractive indices n_D at the operating temperature with found literature values [9–13] as shown in Table 2. The measured densities and refractive indices are in good agreement with the reported literature values, with an average absolute percentage deviation (*AAPD*) of 0.017 % and 0.42 % respectively. The *AAPD* was obtained from Eq. 1:

$$AAPD = \frac{100}{N} \sum_{i=1}^N \frac{|\theta_i^{Exp.} - \theta_i^{Lit.}|}{\theta_i^{Exp.}} \quad (1)$$

where N is the number of experimental data. *Exp.* and *Lit.* are related to experimental value and literature value, respectively, and $\theta = \rho, n_D$.

Table 1 Structure, CAS number, mole fraction purities of the pure compounds and the percentage amount of the 2,3-butanediol stereoisomers

Pure compounds	CAS number	Mole fraction purity	Analysis method ^a
Glycerol	56-81-5	99.0	GC-TCD
1,2-Butanediol	584-03-2	99.0	GC-TCD
1,3-Butanediol	107-88-0	99.0	GC-TCD
1,4-Butanediol	110-63-4	99.0	GC-TCD
2,3-Butanediol	513-85-9	99.0	GC-TCD
(+)-2 S,3 S-Butanediol	–	17.0	GC-FID
(–)-2R,3R-Butanediol	–	15.0	GC-FID
meso-2,3-butanediol	–	66.0	GC-FID

^a Gas-liquid chromatography

Table 2 Experimental densities, ρ , refractive indices, n_D of pure components compared with available literature values at 298.15 K

Component	ρ^a (g·cm ⁻³)		n_D^a	
	Exp.	Lit.	Exp.	Lit.
Glycerol	1.25596	1.25781 [9]	1.471	1.48675 [10]
1,2-Butanediol	0.99825	0.99859 [11]	1.437	1.4364 [11]
1,3-Butanediol	1.00883	1.00532 [12]	1.438	1.439 [12]
1,4-Butanediol	1.01669	1.01304 [12]	1.438	1.446 [13]
2,3-Butanediol	0.98754	0.99858 [11]	1.430	1.436 [12]

^a Standard uncertainties: $u(\rho) = 0.00003$ g·cm⁻³, $u(T) = 0.01$ K for density. $u(n_D) = 0.004$ and $u(P) = 10$ kPa

2.2 Apparatus and Procedure

Electronic densimeter Anton Paar DMA 5000 was deployed to measure densities (ρ) at several different temperatures to an accuracy of $5 \cdot 10^{-6}$ g·cm⁻³. It consists of a borosilicate glass U-tube, 2 mm in diameter and 0.2 mm thick, electronically oscillated at its characteristic frequency. The measurement of the oscillation period of the vibrating tube containing the sample is modified by the mass of the substance introduced, allowing the density of the sample to be determined at the measurement temperature maintained constant to within ± 0.01 K. The densimeter is calibrated periodically using ultrapure water and dry air as reference fluids [14]. The relative standard uncertainty in the density is estimated to be 0.003 %. Refractive index, n_D , were measured with the Abbe-type refractometer Atago Nar-1t Liquid including two Amici compensating prisms, oriented to rotate in opposite directions. It comprises a built-in analog thermometer to display the temperature with an accuracy of ± 0.1 K, it is controlled by a Wise Circu thermostatic bath which is connected to the refractometer by means of a pump circulation. The refractometer is regularly calibrated using commercially available certified standard solutions. The estimated uncertainty of the refractive index is 0.4 %. Measurements were replicated at minimum three times and the results obtained were averaged with a repeatability of 0.1 %. IR spectra were collected via a Perkin Elmer spectrophotometer (model FT-IR two UATR two) at ambient temperature. Mixtures were produced by gravimetric weighing at standard ambient pressure, using an analytical balance (Ohaus, OHAUS00240) to an accuracy of 0.1 mg. The mass fraction standard uncertainty is 0.002. The following propagation error formula was used to evaluate the standard uncertainties for densities and their derivative physical properties [15]:

$$\Delta f^2 = \sum_{j=1}^p \left[\left(\frac{\partial f}{\partial x_j} \right)^2 \Delta x_j^2 \right] \quad (2)$$

The corresponding uncertainty for excess molar volume was calculated using Eq. 3:

$$U_{VE} = \sqrt{\left(\frac{\partial V^E}{\partial d_2}\right)^2_{d,d_1,x_1} U_d^2 + \left(\frac{\partial V^E}{\partial d}\right)^2_{d_1,d_2,x_1} U_d^2 + \left(\frac{\partial V^E}{\partial d_1}\right)^2_{d,d_2,x_1} U_d^2 + \left(\frac{\partial V^E}{\partial x_1}\right)^2_{d,d_1,d_2} U_x^2} \quad (3)$$

where x_1 , d_1 and d_2 denote the mole fractions, and densities of glycerol (1) and butanediol isomer (2), respectively, and d is the density of the mixtures.

3 Theoretical Models

3.1 Modeling for the Density

In this work, the perturbed chain of the statistical associating fluid theory equation of state (PC-SAFT EoS) [16, 17] was used for modeling the density of pure fluids and mixtures. This model has been widely described and used in the literature [18–20]. This equation of state requires five fitted parameters for each pure fluid, which are the following: the number of segments in a chain (m), the segment diameter (σ), the depth of the potential (ε/k_B), the association energy (ε^{AB}/k_B), and the association volume (κ^{AB}). In the above parameters, k_B is the Boltzmann constant.

Due to the presence of three OH groups in glycerol and two OH groups in the butanediol isomers, it is necessary to consider some association scheme. In this manuscript, we have considered one site on each oxygen atom and one site on each hydrogen atom. Therefore, 6 sites have been used on each glycerol molecule, i.e., 3 positive sites and 3 negative sites, and 4 sites on each molecule for butanediol isomers, i.e., 2 positive sites and 2 negative sites. According to this approach, hydrogen bonding is considered between molecules of the same type and between different molecules, that is, self-association and cross-association between molecules.

3.2 Modeling for the Refractive Index

According to the literature, the refractive index for the binary mixture (n_D) can be obtained from Laplace mixing rule [21], using Eq. 4:

$$\frac{n_D^2 - 1}{\rho} = \frac{z_1(n_{D1}^2 - 1)}{\rho_1} + \frac{z_2(n_{D2}^2 - 1)}{\rho_2} \quad (4)$$

where z_1 and z_2 are related to the weight fraction of glycerol and butanediol isomer, respectively. This mixing rule has been used successfully in our recent publications [22, 23]. The liquid density present in Eq. 4 was obtained using PC-SAFT EoS. Therefore, this theoretical approach was named Laplace mixing rule + PC-SAFT EoS.

4 Results and Discussions

4.1 Volumetric Properties

The densities, ρ , and the derivative properties: excess molar volumes, V^E , partial molar volumes, \bar{V}_i , apparent molar volumes, $V_{\phi i}$, isobaric thermal expansion coefficient, α , and excess expansion coefficient, α^E for the glycerol (1) + butanediol isomer (2) binary mixtures at various temperatures (293.15–318.15) K and atmospheric pressure (101325 Pa) over the whole composition range, expressed as the mole fraction, x_1 , of glycerol, are listed in Table 3 and are illustrated in Fig. 1a–d. It can be seen that the V^E values of all mixtures are negative for all compositions and considered temperatures, and the $V^E = f(x_1)$ curves are asymmetric parabola whose extrema correspond to $V_{min}^E = (-0.307, -0.315, -0.323, -0.331, -0.340, -0.350) \text{ cm}^3 \cdot \text{mol}^{-1}$ at $x_1 = 0.5027$ for the mixture with 1,2-butanediol, $V_{min}^E = (-0.026, -0.039, -0.048, -0.057, -0.065, -0.071) \text{ cm}^3 \cdot \text{mol}^{-1}$ at $x_1 = 0.5027$ for the mixture with 1,3-butanediol, $V_{min}^E = (-0.080, -0.079, -0.077, -0.076, -0.074, -0.072) \text{ cm}^3 \cdot \text{mol}^{-1}$ at $x_1 = 0.5985$ for the mixture with 1,4-butanediol and $V_{min}^E = (-0.556, -0.571, -0.585, -0.611, -0.635, -0.658) \text{ cm}^3 \cdot \text{mol}^{-1}$ at $x_1 = 0.5999$ for the mixture with 2,3-butanediol isomer at temperatures $T = (293.15, 298.15, 303.15, 308.15, 313.15, 318.15)$ K respectively for all the mixtures. This compression of the volumes of the binary mixtures ($V^E < 0$) could signify the formation of stronger intermolecular hydrogen bonds between glycerol and the butanediol isomers, or the existence of a greater number of this type of interaction. We also note that the absolute values of $|V^E|$ increase with increasing temperature except for the mixture with 1,4-butanediol.

The excess molar volumes for the mixtures were calculated from the density data of the compositions and pure compounds using the Eq. 5:

$$V^E = \left[\frac{x_1 M_1 + x_2 M_2}{\rho} - \frac{x_1 M_1}{\rho_1} - \frac{x_2 M_2}{\rho_2} \right] \quad (5)$$

where x_1 and x_2 , M_1 and M_2 , and ρ_1 and ρ_2 denote the mole fractions, molar masses, and densities of glycerol (1) and butanediol isomer (2), respectively. ρ , is the density of the mixtures. The experimental V^E values were correlated by least squares polynomial regression to the Redlich-Kister equation [24]:

$$V^E = x_1 x_2 \sum_{i=0}^n A_i (x_1 - x_2)^i \quad (6)$$

The empirical parameters A_i in Eq. 6 are reported in Table S1 along with the standard deviations, σ , expressed as Eq. 7:

Table 3 Experimental densities, ρ , excess molar volumes, V_m^E , partial molar volumes, \bar{V}_ρ , apparent molar volumes, $V_{\phi i}$, isobaric thermal expansion coefficient, α , and excess expansion coefficient, α_E^E , for the glycerol (1) + butanediol isomer (2) mixtures at different temperatures (293.15–318.15 K) and atmospheric pressure (101325 Pa)

x_1	ρ (g·cm $^{-3}$)	V^E (cm 3 ·mol $^{-1}$)	\bar{V}_1 (cm 3 ·mol $^{-1}$)	\bar{V}_2 (cm 3 ·mol $^{-1}$)	V_ϕ (cm 3 ·mol $^{-1}$)	$10^{-3}\alpha$ (K $^{-1}$)	$10^{-6}\alpha^E$ (K $^{-1}$)
Glycerol + 1,2-Butanediol							
293.15 K							
0.000	1.00195	0.000	71.786	89.945	—	89.945	0.000
0.102	1.02497	-0.113	72.312	89.928	72.034	89.819	0.704
0.201	1.04804	-0.201	72.672	89.883	72.141	89.693	0.682
0.302	1.07191	-0.250	72.916	89.816	72.313	89.587	0.650
0.406	1.09770	-0.290	73.070	89.728	72.428	89.456	0.630
0.503	1.12218	-0.307	73.144	89.629	72.531	89.327	0.604
0.602	1.14820	-0.301	73.174	89.507	72.642	89.187	0.580
0.694	1.17255	-0.256	73.176	89.372	72.773	89.107	0.556
0.797	1.20075	-0.198	73.164	89.188	72.893	88.969	0.525
0.897	1.22944	-0.132	73.149	88.962	72.996	88.663	0.498
1.000	1.25905	0.000	73.143	88.668	73.143	—	0.487
298.15 K							
0.000	0.99825	0.000	71.905	90.278	—	90.278	0.745
0.102	1.02135	-0.118	72.468	90.259	72.169	90.147	0.715
0.201	1.04447	-0.208	72.847	90.211	72.287	90.017	0.693
0.302	1.06839	-0.238	73.098	90.143	72.468	89.909	0.661
0.406	1.09424	-0.299	73.252	90.054	72.587	89.774	0.640
0.503	1.11876	-0.315	73.323	89.956	72.695	89.644	0.614
0.602	1.14482	-0.307	73.351	89.835	72.813	89.506	0.589
0.694	1.16924	-0.262	73.352	89.699	72.945	89.422	0.565
0.797	1.19753	-0.204	73.340	89.506	73.067	89.276	0.534
0.897	1.22636	-0.139	73.328	89.260	73.167	88.926	0.507
1.000	1.25596	0.000	73.322	88.927	73.322	—	0.494

Table 3 (continued)

x_1	ρ (g·cm ⁻³)	V^E (cm ³ ·mol ⁻¹)	\bar{V}_1 (cm ³ ·mol ⁻¹)	\bar{V}_2 (cm ³ ·mol ⁻¹)	$V_{\phi 1}$ (cm ³ ·mol ⁻¹)	$V_{\phi 2}$ (cm ³ ·mol ⁻¹)	$10^{-3}\alpha$ (K ⁻¹)	$10^{-6}\alpha^E$ (K ⁻¹)
303.15 K								
0.00	0.99451	0.000	71.980	90.618	—	90.618	0.756	0.000
0.102	1.01767	-0.122	72.608	90.596	72.309	90.482	0.726	-8.528
0.201	1.04084	-0.214	73.020	90.543	72.438	90.349	0.704	-9.310
0.302	1.06482	-0.266	73.283	90.471	72.624	90.237	0.671	-19.422
0.406	1.09070	-0.305	73.438	90.381	72.754	90.104	0.650	-15.404
0.503	1.11530	-0.323	73.506	90.286	72.862	89.968	0.624	-18.080
0.602	1.14140	-0.314	73.530	90.169	72.985	89.829	0.599	-17.515
0.694	1.16592	-0.270	73.529	90.035	73.117	89.736	0.574	-17.803
0.797	1.19432	-0.213	73.518	89.836	73.238	89.571	0.542	-20.602
0.897	1.22326	-0.148	73.508	89.568	73.340	89.175	0.515	-18.707
1.000	1.25284	0.000	73.505	89.187	73.505	—	0.502	0.000
308.15 K								
0.00	0.99073	0.000	72.089	90.964	—	90.964	0.767	0.000
0.102	1.01395	-0.126	72.755	90.940	72.456	90.823	0.737	-8.449
0.201	1.03715	-0.219	73.188	90.884	72.602	90.690	0.715	-9.214
0.302	1.06121	-0.274	73.464	90.808	72.783	90.572	0.681	-19.258
0.406	1.08713	-0.313	73.623	90.715	72.921	90.437	0.660	-15.257
0.503	1.11171	-0.331	73.692	90.619	73.032	90.297	0.633	-17.921
0.602	1.13799	-0.323	73.715	90.502	73.154	90.150	0.608	-17.350
0.694	1.16257	-0.279	73.714	90.366	73.290	90.053	0.583	-17.653
0.797	1.19109	-0.223	73.703	90.164	73.411	89.867	0.551	-20.446
0.897	1.22004	-0.153	73.694	89.887	73.521	89.476	0.523	-18.609
1.000	1.24968	0.000	73.691	89.488	73.691	—	0.510	0.000

Table 3 (continued)

x_1	ρ (g·cm $^{-3}$)	V^E (cm 3 ·mol $^{-1}$)	\bar{V}_1 (cm 3 ·mol $^{-1}$)	\bar{V}_2 (cm 3 ·mol $^{-1}$)	$V_{\phi 1}$ (cm 3 ·mol $^{-1}$)	$V_{\phi 2}$ (cm 3 ·mol $^{-1}$)	$10^{-3}\alpha$ (K $^{-1}$)	$10^{-6}\alpha^E$ (K $^{-1}$)
313.15 K								
0.00	0.98691	0.000	72.198	91.316	91.316	0.778	0.000	
0.102	1.01020	-0.130	72.906	91.290	72.604	91.171	0.748	-8.366
0.201	1.03340	-0.222	73.362	91.230	72.776	91.038	0.725	-9.129
0.302	1.05760	-0.285	73.649	91.151	72.937	90.908	0.692	-19.069
0.406	1.08356	-0.323	73.813	91.056	73.086	90.772	0.670	-15.087
0.503	1.10826	-0.340	73.882	90.959	73.204	90.632	0.643	-17.756
0.602	1.13451	-0.332	73.904	90.841	73.330	90.481	0.617	-17.192
0.694	1.15916	-0.287	73.901	90.704	73.468	90.378	0.592	-17.508
0.797	1.18778	-0.231	73.891	90.497	73.591	90.178	0.559	-20.302
0.897	1.21686	-0.162	73.883	90.208	73.700	89.739	0.531	-18.477
1.000	1.24647	0.000	73.881	89.783	73.881	0.517	0.000	
318.15 K								
0.00	0.98305	0.000	72.314	91.674	—	91.674	0.789	0.000
0.102	1.00640	-0.134	73.063	91.646	72.755	91.525	0.759	-8.284
0.201	1.02963	-0.226	73.542	91.583	72.950	91.391	0.735	-9.037
0.302	1.05395	-0.297	73.840	91.501	73.090	91.249	0.702	-18.872
0.406	1.07986	-0.326	74.006	91.405	73.270	91.124	0.680	-14.970
0.503	1.10469	-0.350	74.074	91.308	73.377	90.970	0.653	-17.581
0.602	1.13100	-0.340	74.094	91.190	73.508	90.818	0.626	-17.036
0.694	1.15571	-0.294	74.091	91.053	73.650	90.713	0.601	-17.367
0.797	1.18443	-0.239	74.080	90.840	73.773	90.497	0.568	-20.160
0.897	1.21360	-0.169	74.074	90.536	73.885	90.032	0.539	-18.361
1.000	1.24323	0.000	74.073	90.082	74.073	—	0.525	0.000

Table 3 (continued)

x_1	ρ (g·cm ⁻³)	V^E (cm ³ ·mol ⁻¹)	\bar{V}_1 (cm ³ ·mol ⁻¹)	\bar{V}_2 (cm ³ ·mol ⁻¹)	$V_{\phi 1}$ (cm ³ ·mol ⁻¹)	$V_{\phi 2}$ (cm ³ ·mol ⁻¹)	$10^{-3}\alpha$ (K ⁻¹)	$10^{-6}\alpha^E$ (K ⁻¹)
Glycerol + 1,3-Butanediol								
293.15 K								
0.000	1.01225	0.000	73.140	89.029	—	89.029	0.670	0.000
0.099	1.03264	-0.004	73.105	89.032	73.099	89.024	0.650	-5.522
0.200	1.05436	-0.011	73.099	89.034	73.090	89.016	0.628	-10.884
0.314	1.07991	-0.018	73.112	89.031	73.086	89.004	0.603	-16.839
0.401	1.10019	-0.025	73.127	89.022	73.081	88.988	0.584	-21.082
0.500	1.12395	-0.026	73.143	89.005	73.091	88.978	0.566	-21.925
0.598	1.14840	-0.022	73.153	88.985	73.105	88.974	0.548	-21.059
0.701	1.17488	-0.016	73.157	88.966	73.120	88.975	0.531	-18.792
0.799	1.20128	-0.011	73.153	88.958	73.129	88.976	0.516	-13.726
0.898	1.22926	-0.004	73.147	88.970	73.138	88.989	0.502	-6.989
1.000	1.25905	0.000	73.143	89.019	73.143	—	0.487	0.000
298.15 K								
0.000	1.00883	0.000	73.331	89.331	—	89.331	0.682	0.000
0.099	1.02925	-0.006	73.273	89.335	73.259	89.324	0.661	-5.489
0.200	1.05102	-0.016	73.260	89.339	73.244	89.312	0.640	-10.811
0.314	1.07664	-0.026	73.276	89.335	73.240	89.294	0.614	-16.725
0.401	1.09697	-0.035	73.298	89.322	73.235	89.273	0.595	-20.943
0.500	1.12081	-0.039	73.322	89.298	73.245	89.254	0.576	-21.766
0.598	1.14525	-0.032	73.338	89.267	73.268	89.250	0.558	-20.924
0.701	1.17172	-0.023	73.344	89.239	73.290	89.255	0.540	-18.693
0.799	1.19812	-0.013	73.339	89.226	73.306	89.265	0.525	-13.671
0.898	1.22615	-0.006	73.328	89.245	73.315	89.268	0.510	-6.955

Table 3 (continued)

x_1	ρ (g·cm $^{-3}$)	V^E (cm 3 ·mol $^{-1}$)	\bar{V}_1 (cm 3 ·mol $^{-1}$)	\bar{V}_2 (cm 3 ·mol $^{-1}$)	$V_{\phi 1}$ (cm 3 ·mol $^{-1}$)	$V_{\phi 2}$ (cm 3 ·mol $^{-1}$)	$10^{-3}\alpha$ (K $^{-1}$)	$10^{-6}\alpha^E$ (K $^{-1}$)
1.000	1.25596	0.000	73.322	89.319	73.322	—	0.494	0.000
303.15 K								
0.000	1.00537	0.000	73.494	89.639	—	89.639	0.694	0.000
0.099	1.02582	-0.008	73.433	89.643	73.428	89.630	0.673	-5.459
0.200	1.04763	-0.019	73.424	89.647	73.407	89.614	0.651	-10.744
0.314	1.07330	-0.032	73.448	89.641	73.403	89.592	0.625	-16.622
0.401	1.09368	-0.043	73.476	89.624	73.397	89.567	0.605	-20.813
0.500	1.11756	-0.048	73.505	89.594	73.409	89.543	0.586	-21.629
0.598	1.14205	-0.042	73.524	89.558	73.435	89.534	0.568	-20.792
0.701	1.16853	-0.029	73.531	89.524	73.463	89.541	0.549	-18.592
0.799	1.19496	-0.019	73.525	89.509	73.481	89.544	0.534	-13.592
0.898	1.22300	-0.009	73.513	89.533	73.495	89.551	0.518	-6.919
1.000	1.25284	0.000	73.505	89.621	73.505	—	0.502	0.000
308.15 K								
0.000	1.00186	0.000	73.636	89.953	—	89.953	0.706	0.000
0.099	1.02235	-0.010	73.591	89.957	73.586	89.942	0.684	-5.418
0.200	1.04420	-0.024	73.593	89.959	73.570	89.923	0.662	-10.670
0.314	1.06992	-0.039	73.626	89.950	73.567	89.896	0.636	-16.512
0.401	1.09034	-0.051	73.659	89.931	73.563	89.867	0.616	-20.683
0.500	1.11426	-0.057	73.691	89.897	73.578	89.840	0.596	-21.493
0.598	1.13877	-0.050	73.712	89.858	73.608	89.830	0.577	-20.670
0.701	1.16553	-0.039	73.718	89.820	73.635	89.822	0.558	-18.465
0.799	1.19177	-0.026	73.712	89.802	73.659	89.826	0.542	-13.507
0.898	1.21981	-0.012	73.699	89.823	73.678	89.837	0.527	-6.880

Table 3 (continued)

x_1	ρ (g·cm ⁻³)	V^E (cm ³ ·mol ⁻¹)	\bar{V}_1 (cm ³ ·mol ⁻¹)	\bar{V}_2 (cm ³ ·mol ⁻¹)	$V_{\phi 1}$ (cm ³ ·mol ⁻¹)	$V_{\phi 2}$ (cm ³ ·mol ⁻¹)	$10^{-3}\alpha$ (K ⁻¹)	$10^{-6}\alpha^E$ (K ⁻¹)
1.000	1.24968	0.000	73.691	89.909	73.691	—	0.510	0.000
313.15 K								
0.000	0.99830	0.000	73.799	90.274	—	90.274	0.717	0.000
0.099	1.01883	-0.013	73.760	90.277	73.751	90.259	0.695	-5.379
0.200	1.04072	-0.029	73.766	90.279	73.737	90.238	0.673	-10.595
0.314	1.06650	-0.046	73.809	90.268	73.733	90.206	0.646	-16.397
0.401	1.08696	-0.060	73.845	90.246	73.731	90.173	0.626	-20.543
0.500	1.11091	-0.065	73.881	90.210	73.751	90.144	0.606	-21.359
0.598	1.13545	-0.057	73.903	90.165	73.786	90.132	0.587	-20.549
0.701	1.16204	-0.046	73.910	90.123	73.816	90.120	0.567	-18.359
0.799	1.18852	-0.032	73.903	90.101	73.841	90.117	0.551	-13.424
0.898	1.21657	-0.014	73.889	90.118	73.865	90.135	0.535	-6.844
1.000	1.24647	0.000	73.881	90.202	73.881	—	0.517	0.000
318.15 K								
0.000	0.99470	0.000	73.962	90.601	—	90.601	0.729	0.000
0.099	1.01528	-0.017	73.936	90.604	73.903	90.582	0.706	-5.327
0.200	1.03721	-0.035	73.953	90.605	73.900	90.557	0.683	-10.510
0.314	1.06304	-0.054	73.999	90.592	73.902	90.522	0.657	-16.280
0.401	1.08354	-0.070	74.037	90.570	73.900	90.484	0.636	-20.399
0.500	1.10748	-0.071	74.073	90.531	73.931	90.459	0.616	-21.238
0.598	1.13209	-0.065	74.096	90.484	73.964	90.438	0.596	-20.419
0.701	1.15871	-0.052	74.102	90.436	73.999	90.427	0.576	-18.255
0.799	1.18521	-0.035	74.095	90.407	74.029	90.425	0.559	-13.354
0.898	1.21331	-0.017	74.082	90.414	74.054	90.430	0.543	-6.801

Table 3 (continued)

x_1	ρ ($\text{g}\cdot\text{cm}^{-3}$)	V^E ($\text{cm}^3\cdot\text{mol}^{-1}$)	\bar{V}_1 ($\text{cm}^3\cdot\text{mol}^{-1}$)	\bar{V}_2 ($\text{cm}^3\cdot\text{mol}^{-1}$)	$V_{\phi 1}$ ($\text{cm}^3\cdot\text{mol}^{-1}$)	$V_{\phi 2}$ ($\text{cm}^3\cdot\text{mol}^{-1}$)	$10^{-3}\alpha$ (K^{-1})	$10^{-6}\alpha^E$ (K^{-1})
1.00	1.24323	0.000	74.073	90.483	74.073	—	0.525	0.000
293.15 K								
Glycerol + 1,4-Butanediol								
0.000	1.01976	0.000	72.741	88.374	—	88.374	0.599	0.000
0.100	1.04023	-0.024	72.888	88.369	72.899	88.347	0.593	3.144
0.200	1.06135	-0.042	72.995	88.354	72.931	88.321	0.585	4.747
0.399	1.10565	-0.070	73.116	88.306	72.967	88.257	0.565	5.349
0.503	1.12993	-0.079	73.143	88.276	72.985	88.215	0.554	5.629
0.599	1.15310	-0.080	73.154	88.247	73.008	88.174	0.542	4.577
0.700	1.17839	-0.070	73.155	88.216	73.043	88.143	0.530	4.954
0.800	1.20432	-0.057	73.151	88.186	73.071	88.088	0.518	4.910
0.899	1.23116	-0.036	73.145	88.157	73.102	88.013	0.503	3.137
1.000	1.25905	0.000	73.143	88.129	73.143	—	0.487	0.000
298.15 K								
0.000	1.01669	0.000	72.936	88.641	—	88.641	0.604	0.000
0.100	1.03714	-0.023	73.073	88.635	73.095	88.615	0.598	3.125
0.200	1.05825	-0.041	73.176	88.621	73.119	88.590	0.590	4.725
0.301	1.08019	-0.057	73.248	88.600	73.132	88.559	0.579	3.902
0.399	1.10252	-0.068	73.295	88.574	73.152	88.527	0.571	5.323
0.503	1.12680	-0.077	73.323	88.544	73.168	88.485	0.560	5.608
0.599	1.14996	-0.079	73.334	88.515	73.191	88.445	0.548	4.560
0.700	1.17525	-0.068	73.336	88.484	73.225	88.414	0.537	4.935
0.800	1.20120	-0.056	73.331	88.457	73.252	88.361	0.525	4.894
0.899	1.22804	-0.035	73.325	88.432	73.283	88.293	0.511	3.124

Table 3 (continued)

x_1	ρ (g·cm ⁻³)	V^E (cm ³ ·mol ⁻¹)	\bar{V}_1 (cm ³ ·mol ⁻¹)	\bar{V}_2 (cm ³ ·mol ⁻¹)	$V_{\phi 1}$ (cm ³ ·mol ⁻¹)	$V_{\phi 2}$ (cm ³ ·mol ⁻¹)	$10^{-3}\alpha$ (K ⁻¹)	$10^{-6}\alpha^E$ (K ⁻¹)
1.000	1.25596	0.000	73.322	88.413	73.322	—	0.494	0.000
303.15 K								
0.000	1.01361	0.000	73.135	88.910	—	88.910	0.609	0.000
0.100	1.03403	-0.022	73.262	88.905	73.289	88.886	0.603	3.109
0.200	1.05512	-0.039	73.360	88.892	73.309	88.861	0.596	4.703
0.301	1.07705	-0.056	73.430	88.871	73.319	88.830	0.585	3.886
0.399	1.09936	-0.066	73.477	88.845	73.340	88.800	0.576	5.298
0.503	1.12364	-0.076	73.506	88.815	73.354	88.757	0.566	5.588
0.599	1.14680	-0.077	73.518	88.785	73.376	88.717	0.555	4.545
0.700	1.17208	-0.067	73.519	88.755	73.410	88.688	0.544	4.919
0.800	1.19803	-0.055	73.515	88.729	73.437	88.638	0.532	4.876
0.899	1.22488	-0.034	73.508	88.709	73.468	88.576	0.518	3.110
1.000	1.25284	0.000	73.505	88.698	73.505	—	0.502	0.000
308.15 K								
0.000	1.01052	0.000	73.329	89.182	—	89.182	0.614	0.000
0.100	1.03091	-0.021	73.453	89.177	73.481	89.159	0.608	3.097
0.200	1.05197	-0.037	73.548	89.164	73.504	89.135	0.601	4.679
0.301	1.07390	-0.054	73.617	89.144	73.510	89.104	0.591	3.868
0.399	1.09618	-0.064	73.663	89.118	73.530	89.075	0.582	5.277
0.503	1.12045	-0.074	73.692	89.088	73.544	89.033	0.572	5.565
0.599	1.14361	-0.076	73.704	89.059	73.564	88.992	0.561	4.529
0.700	1.16889	-0.065	73.706	89.030	73.598	88.965	0.550	4.901
0.800	1.19483	-0.053	73.701	89.005	73.625	88.918	0.539	4.856
0.899	1.22170	-0.033	73.695	88.988	73.654	88.850	0.525	3.104

Table 3 (continued)

x_1	ρ (g·cm ⁻³)	V^E (cm ³ ·mol ⁻¹)	\bar{V}_1 (cm ³ ·mol ⁻¹)	\bar{V}_2 (cm ³ ·mol ⁻¹)	$V_{\phi 1}$ (cm ³ ·mol ⁻¹)	$V_{\phi 2}$ (cm ³ ·mol ⁻¹)	$10^{-3}\alpha$ (K ⁻¹)	$10^{-6}\alpha^E$ (K ⁻¹)
1.000	1.24968	0.000	73.691	88.981	73.691	—	0.510	0.000
313.15 K								
0.000	1.00741	0.000	73.539	89.457	—	89.457	0.619	0.000
0.100	1.02776	-0.019	73.651	89.453	73.689	89.436	0.613	3.076
0.200	1.04880	-0.035	73.739	89.441	73.705	89.413	0.606	4.652
0.301	1.07071	-0.053	73.806	89.421	73.706	89.382	0.596	3.848
0.399	1.09298	-0.062	73.852	89.396	73.725	89.353	0.588	5.253
0.503	1.11722	-0.071	73.882	89.365	73.739	89.314	0.578	5.535
0.599	1.14038	-0.074	73.894	89.336	73.757	89.273	0.567	4.509
0.700	1.16565	-0.063	73.897	89.307	73.791	89.247	0.557	4.879
0.800	1.19159	-0.051	73.892	89.285	73.817	89.203	0.546	4.834
0.899	1.21847	-0.032	73.885	89.273	73.845	89.140	0.532	3.088
1.000	1.24647	0.000	73.881	89.278	73.881	—	0.517	0.000
318.15 K								
0.000	1.00428	0.000	73.754	89.736	—	89.736	0.624	0.000
0.100	1.02459	-0.018	73.853	89.732	73.898	89.716	0.618	3.056
0.200	1.04560	-0.033	73.934	89.721	73.910	89.695	0.611	4.622
0.301	1.06751	-0.051	73.999	89.702	73.903	89.663	0.602	3.829
0.399	1.08975	-0.060	74.044	89.677	73.923	89.636	0.594	5.224
0.503	1.11397	-0.069	74.074	89.646	73.936	89.597	0.584	5.506
0.599	1.13713	-0.072	74.087	89.617	73.953	89.556	0.574	4.488
0.700	1.16238	-0.060	74.090	89.588	73.987	89.535	0.563	4.851
0.800	1.18832	-0.049	74.085	89.568	74.012	89.493	0.553	4.810
0.899	1.21521	-0.031	74.077	89.562	74.039	89.431	0.540	3.074

Table 3 (continued)

x_1	ρ (g·cm ⁻³)	V^E (cm ³ ·mol ⁻¹)	\bar{V}_1 (cm ³ ·mol ⁻¹)	\bar{V}_2 (cm ³ ·mol ⁻¹)	$V_{\phi 1}$ (cm ³ ·mol ⁻¹)	$V_{\phi 2}$ (cm ³ ·mol ⁻¹)	$10^{-3}\alpha$ (K ⁻¹)	$10^{-6}\alpha^E$ (K ⁻¹)
1.000	1.24323	0.000	74.073	89.578	74.073	—	0.525	0.000
Glycerol + 2,3-Butanediol								
293.15 K								
0.000	0.99175	0.000	69.227	90.869	—	90.869	0.846	0.000
0.104	1.01684	-0.197	71.097	90.786	71.247	90.649	-1.899	-27.134
0.200	1.04091	-0.360	72.158	90.623	71.347	90.419	-4.188	-49.731
0.299	1.06558	-0.437	72.767	90.443	71.683	90.246	-5.478	-62.320
0.400	1.09127	-0.484	73.053	90.288	71.931	90.063	-6.380	-71.005
0.502	1.11896	-0.544	73.143	90.168	72.060	89.777	-7.266	-79.503
0.600	1.14586	-0.556	73.139	90.070	72.216	89.480	-7.605	-82.545
0.704	1.17529	-0.535	73.114	89.924	72.382	89.063	-7.249	-78.594
0.799	1.20251	-0.464	73.107	89.673	72.561	88.567	-6.436	-70.082
0.900	1.23174	-0.321	73.125	89.164	72.786	87.677	-4.336	-48.664
1.000	1.25905	0.000	73.143	88.260	73.143	—	0.487	0.000
298.15 K								
0.000	0.98755	0.000	69.317	91.257	—	91.257	0.857	0.000
0.104	1.01278	-0.206	71.237	91.171	71.344	91.027	-1.877	-27.025
0.200	1.03696	-0.374	72.323	91.006	71.455	90.789	-4.158	-49.540
0.299	1.06177	-0.457	72.944	90.823	71.797	90.605	-5.445	-62.095
0.400	1.08760	-0.507	73.234	90.665	72.054	90.413	-6.346	-70.763
0.502	1.11526	-0.556	73.323	90.544	72.214	90.139	-7.229	-79.238
0.600	1.14231	-0.571	73.316	90.441	72.370	89.829	-7.570	-82.287
0.704	1.17189	-0.550	73.290	90.286	72.540	89.399	-7.218	-78.364
0.799	1.19922	-0.476	73.284	90.017	72.726	88.895	-6.408	-69.889

Table 3 (continued)

x_1	ρ (g·cm $^{-3}$)	V^E (cm 3 ·mol $^{-1}$)	\bar{V}_1 (cm 3 ·mol $^{-1}$)	\bar{V}_2 (cm 3 ·mol $^{-1}$)	$V_{\phi 1}$ (cm 3 ·mol $^{-1}$)	$V_{\phi 2}$ (cm 3 ·mol $^{-1}$)	$10^{-3}\alpha$ (K $^{-1}$)	$10^{-6}\alpha^E$ (K $^{-1}$)
303.15 K	0.900	1.22856	-0.329	73.304	89.474	72.957	87.988	-4.315
	1.000	1.25596	0.000	73.322	88.513	73.322	-	0.494
	0.000	0.98329	0.000	69.433	91.651	-	91.651	0.000
	0.104	1.00866	-0.215	71.381	91.565	71.440	91.411	-1.855
	0.200	1.03297	-0.389	72.485	91.398	71.564	91.165	-4.128
	0.299	1.05791	-0.476	73.117	91.213	71.916	90.972	-5.412
	0.400	1.08386	-0.529	73.413	91.051	72.181	90.771	-6.311
	0.502	1.11165	-0.579	73.506	90.924	72.351	90.487	-7.194
	0.600	1.13870	-0.585	73.500	90.813	72.530	90.189	-7.534
	0.704	1.16843	-0.565	73.474	90.644	72.703	89.745	-7.185
308.15 K	0.799	1.19588	-0.488	73.468	90.358	72.894	89.230	-6.380
	0.900	1.22535	-0.336	73.487	89.790	73.131	88.304	-4.294
	1.000	1.25284	0.000	73.505	88.794	73.505	-	0.502
	0.000	0.97901	0.000	69.566	92.053	-	92.053	0.000
	0.104	1.00451	-0.224	71.522	91.967	71.539	91.803	-1.833
	0.200	1.02893	-0.404	72.637	91.800	71.677	91.548	-4.098
	0.299	1.05399	-0.494	73.283	91.611	72.040	91.347	-5.379
	0.400	1.08007	-0.550	73.591	91.443	72.314	91.137	-6.276
	0.502	1.10800	-0.603	73.692	91.304	72.491	90.842	-7.158
	0.600	1.13521	-0.611	73.691	91.180	72.673	90.526	-7.500
	0.704	1.16493	-0.579	73.666	90.996	72.868	90.097	-7.153
	0.799	1.19249	-0.499	73.658	90.696	73.066	89.574	-6.351

Table 3 (continued)

x_1	ρ (g·cm ⁻³)	V^E (cm ³ ·mol ⁻¹)	\bar{V}_1 (cm ³ ·mol ⁻¹)	\bar{V}_2 (cm ³ ·mol ⁻¹)	$V_{\phi 1}$ (cm ³ ·mol ⁻¹)	$V_{\phi 2}$ (cm ³ ·mol ⁻¹)	$10^{-3}\alpha$ (K ⁻¹)	$10^{-6}\alpha^E$ (K ⁻¹)
313.15 K								
0.900	1.22208	-0.344	73.675	90.117	73.309	88.634	-4.273	-48.279
1.000	1.24968	0.000	73.691	89.119	73.691	-	0.510	0.000
0.000	0.97469	0.000	69.707	92.460	-	92.460	0.889	0.000
0.104	1.00033	-0.232	71.672	92.375	71.650	92.201	-1.811	-26.689
0.200	1.02487	-0.418	72.798	92.207	71.794	91.937	-4.068	-48.957
0.299	1.05004	-0.512	73.455	92.015	72.169	91.729	-5.346	-61.402
0.400	1.07624	-0.571	73.773	91.842	72.452	91.509	-6.242	-70.017
0.502	1.10430	-0.625	73.882	91.693	72.636	91.204	-7.122	-78.451
0.600	1.13165	-0.635	73.885	91.557	72.822	90.873	-7.465	-81.512
0.704	1.16133	-0.590	73.861	91.358	73.043	90.469	-7.120	-77.653
0.799	1.18907	-0.512	73.852	91.044	73.240	89.919	-6.323	-69.293
0.900	1.21876	-0.350	73.866	90.452	73.491	88.973	-4.252	-48.147
1.000	1.24647	0.000	73.881	89.446	73.881	-	0.517	0.000
318.15 K								
0.000	0.97034	0.000	69.720	92.875	-	92.875	0.900	0.000
0.104	0.99611	-0.241	71.773	92.786	71.754	92.605	-1.789	-26.576
0.200	1.02076	-0.433	72.948	92.610	71.914	92.333	-4.038	-48.759
0.299	1.04605	-0.531	73.632	92.410	72.300	92.117	-5.312	-61.167
0.400	1.07237	-0.592	73.962	92.230	72.592	91.889	-6.206	-69.763
0.502	1.10056	-0.648	74.074	92.078	72.783	91.573	-7.086	-78.183
0.600	1.12804	-0.658	74.077	91.939	72.976	91.230	-7.429	-81.249
0.704	1.15787	-0.612	74.051	91.734	73.203	90.808	-7.088	-77.419
0.799	1.18577	-0.535	74.042	91.410	73.404	90.222	-6.295	-69.098

Table 3 (continued)

x_1	ρ (g·cm $^{-3}$)	V^E (cm 3 ·mol $^{-1}$)	\bar{V}_1 (cm 3 ·mol $^{-1}$)	\bar{V}_2 (cm 3 ·mol $^{-1}$)	$V_{\phi 1}$ (cm 3 ·mol $^{-1}$)	$V_{\phi 2}$ (cm 3 ·mol $^{-1}$)	$10^{-3}\alpha$ (K $^{-1}$)	$10^{-6}\alpha^E$ (K $^{-1}$)
0.900	1.21551	-0.363	74.057	90.794	73.669	89.261	-4.231	-48.017
1.000	1.24323	0.000	74.073	89.745	74.073	-	0.525	0.000

Standard uncertainties: $u(x_1) = 0.002$, $u(\rho) = 0.00003$ g·cm $^{-3}$, $u(V^E) = 0.15 \cdot 10^{-3}$ cm 3 ·mol $^{-1}$, $u(T) = 0.01$ K, $u(\bar{V}_i) = u(\bar{V}_i) = u(V_{\phi i}) = 9 \cdot 10^{-3}$ cm 3 ·mol $^{-1}$, $u(P) = 10$ kPa, $u(\alpha) = u(\alpha^E) = 5 \cdot 10^{-2}$ K $^{-1}$

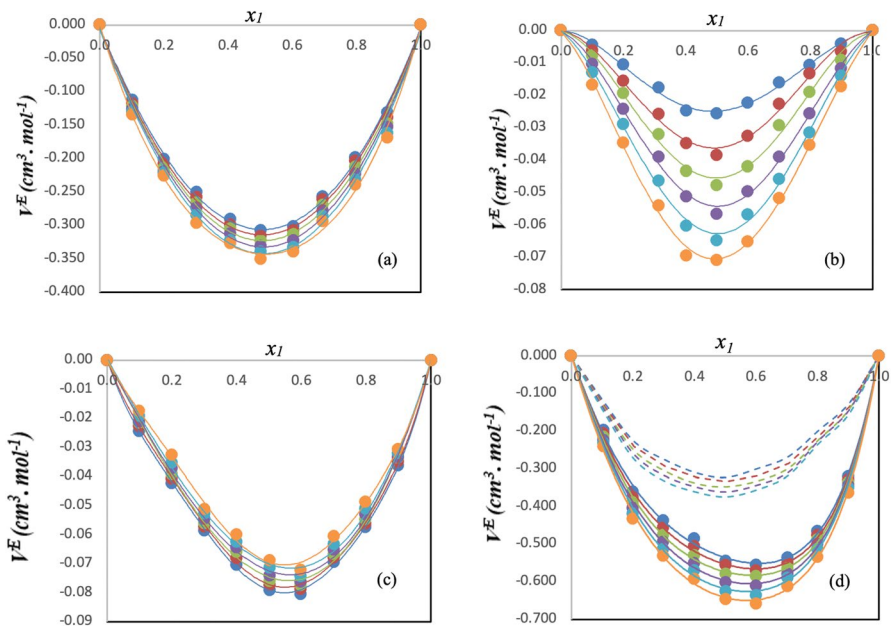


Fig. 1 Excess molar volumes of glycerol (1) + butanediol isomer (2) mixtures at $T = [298.15\text{--}318.15]\text{ K}$ and atmospheric pressure: (a) glycerol (1) + 1,2-butanediol (2) mixture, (b) glycerol (1) + 1,3-butanediol (2) mixture, (c) glycerol (1) + 1,4-butanediol (2) mixture, (d) glycerol (1) + 2,3-butanediol (2) mixture. Circles: experimental data obtained in this work. Colors: (orange) 293.15 K, (sky blue) 298.15 K, (purple) 303.15 K, (green) 308.15 K, (red) 313.15, (blue) 318.15 K. Continuous line: represent the results obtained with RK polynomial. Segmented line: represent the results obtained by Alavianmehr et al. [25] (Color figure online)

$$\sigma = \left[\frac{\sum_{i=1}^N (V_{exp,i}^E - V_{calc,i}^E)^2}{N - n} \right]^{1/2} \quad (7)$$

where N is the number of measurements and n the number of fitted parameters A_i . Figure 1 shows the experimental values of excess molar volume, V^E , as a function of glycerol mole fraction, x_1 , along with adjusted curves calculated using Eq. 6, at chosen temperature range from (293.15 to 318.15) K.

The same trend was observed in the results previously published by Alavianmehr et al. [25] concerning the binary mixture glycerol + 2,3-butanediol for the densities, ρ and the excess molar volumes, V^E , at the five temperatures: 298.15 K, 303.15 K, 308.15 K, 313.15 K, and 318.15 K. The estimated average absolute percentage deviations (AAPD) for the densities equals 0.68 %. However, for the excess molar volumes, V^E , AAPD = 45 %. The difference in the enantiomeric composition of 2,3-butanediol could potentially be the source of the deviations

between our results and those reported in the literature [25]. However, no such enantiomeric analysis is provided in this reference to further investigate this aspect (Fig. 1).

The partial molar volumes, \bar{V}_1 and \bar{V}_2 , for glycerol (1) and butanediol isomer (2), respectively, were investigated over the entire composition range by means of the Eqs. 8, 9:

$$\bar{V}_1 = V^E + V_1^0 + (1 - x_1) \left(\frac{\partial V^E}{\partial x_1} \right)_{T,P} \quad (8)$$

$$\bar{V}_2 = V^E + V_2^0 + x_1 \left(\frac{\partial V^E}{\partial x_1} \right)_{T,P} \quad (9)$$

where V_1^0 and V_2^0 are the molar volumes of pure liquid components 1 and 2, respectively. Differentiation of V^E from Eq. 7 with respect to x_1 and substitution of the results in Eqs. 8, 9 gives rise to the following Eqs. 10, 11 for the partial molar volumes \bar{V}_1 and \bar{V}_2 :

$$\bar{V}_1 = V_1^0 + (1 - x_1)^2 \sum_{i=0}^n A_i (1 - 2x_1)^i - 2x_1 (1 - x_1)^2 \sum_{i=0}^n A_i (i) (1 - 2x_1)^{i-1} \quad (10)$$

$$\bar{V}_2 = V_2^0 + x_1^2 \sum_{i=0}^n A_i (1 - 2x_1)^i - 2x_1^2 (1 - x_1) \sum_{i=0}^n A_i (i) (1 - 2x_1)^{i-1} \quad (11)$$

Assigning $x_1 = 0$ in Eq. 10 and $x_2 = 0$ in Eq. 11 generates the Eqs. 12, 13, for the partial molar volume of glycerol at infinite dilution, \bar{V}_1^∞ , in the butanol and the partial molar volume of the butanol at infinite dilution, \bar{V}_2^∞ , in glycerol:

$$\bar{V}_1^\infty = V_1^0 + \sum_{i=0}^n A_i \quad (12)$$

$$\bar{V}_2^\infty = V_2^0 + \sum_{i=0}^n A_i (i)^{-1} \quad (13)$$

Reordering of Eqs. 12, 13 leads to Eqs. 14, 15, for the partial excess molar volume of glycerol at infinite dilution, $\bar{V}_1^{E\infty}$, in the butanol, and the partial molar volume of the butanol at infinite dilution, $\bar{V}_2^{E\infty}$, in glycerol, respectively,

$$\bar{V}_1^{E\infty} = \sum_{i=0}^n A_i \quad (14)$$

Table 4 Limiting partial molar volumes, \overline{V}_1^∞ and \overline{V}_2^∞ , and limiting excess partial molar volume $\overline{V}_1^{E\infty}$ of glycerol and for butanediol isomer $\overline{V}_2^{E\infty}$, for the four binary mixtures: glycerol (1) + butanediol isomer (2) mixtures at different temperatures (293.15–318.15) K and atmospheric pressure (101325 Pa)

T (K)	\overline{V}_1^∞ (cm ³ ·mol ⁻¹)	\overline{V}_2^∞ (cm ³ ·mol ⁻¹)	$\overline{V}_1^{E\infty}$ (cm ³ ·mol ⁻¹)	$\overline{V}_2^{E\infty}$ (cm ³ ·mol ⁻¹)
Glycerol + 1,2-Butanediol				
293.15	71.79	89.75	−1.36	−0.09
298.15	71.91	90.06	−1.42	−0.11
303.15	71.98	90.36	−1.53	−0.15
308.15	72.09	90.67	−1.60	−0.18
313.15	72.20	91.00	−1.68	−0.21
318.15	72.31	91.33	−1.76	−0.24
Glycerol + 1,3-Butanediol				
293.15	73.14	89.08	−0.00	0.05
298.15	73.33	89.41	0.01	0.08
303.15	73.49	89.73	−0.01	0.09
308.15	73.64	90.03	−0.06	0.08
313.15	73.80	90.36	−0.08	0.08
318.15	73.96	90.69	−0.11	0.09
Glycerol + 1,4-Butanediol				
293.15	72.74	88.29	−0.40	−0.08
298.15	72.94	88.56	−0.39	−0.08
303.15	73.14	88.83	−0.37	−0.08
308.15	73.33	89.11	−0.36	−0.08
313.15	73.54	89.39	−0.34	−0.07
318.15	73.75	89.67	−0.32	−0.06
Glycerol + 2,3-Butanediol				
293.15	69.23	89.66	−3.92	−1.21
298.15	69.32	90.04	−4.01	−1.21
303.15	69.43	90.46	−4.07	−1.19
308.15	69.57	90.88	−4.13	−1.17
313.15	69.71	91.32	−4.17	−1.14
318.15	69.72	91.67	−4.35	−1.20

Standard uncertainties: $u(x_1) = 0.002$, $u(\overline{V}_i^\infty) = u(\overline{V}_i^{E\infty}) = 5 \cdot 10^{-2} \text{ cm}^3 \cdot \text{mol}^{-1}$

$$\overline{V}_1^{E\infty} = \sum_{i=0}^n A_i(i)^{-1} \quad (15)$$

Partial molar volumes, \overline{V}_i , are listed in Table 3, partial molar volumes at infinite dilution, \overline{V}_i^∞ , and partial molar excess volumes at infinite dilution, $\overline{V}_i^{E\infty}$, were determined at some temperatures ranging from (298.15 to 318.15) K, using the empirical parameters A_i given in Table S1. The partial properties at infinite dilution are of

considerable attention since the solute-solute interactions disappear in this region and the only interactions remaining are solute-solvent [26]. Thus, the values of partial molar volumes at infinite dilution provide insight into solute-solvent interactions. The partial molar volumes at infinite dilution and partial molar excess volumes at infinite dilution are listed in Table 4.

The apparent molar volumes of glycerol in butanol, $V_{\phi 1}$, and the apparent molar volume of butanol in glycerol, $V_{\phi 2}$, are given by the following equations:

$$V_{\phi 1} = \frac{V - x_2 V_2^0}{x_1} \quad (16)$$

$$V_{\phi 2} = \frac{V - x_1 V_1^0}{x_2} \quad (17)$$

where the molar volume of the binary system, V , is expressed by:

$$V = V^E + x_1 V_1^0 + x_2 V_2^0 \quad (18)$$

Combining the Eqs. 16, 17, 18 mains to Eqs. 19, 20, for the apparent molar volumes $V_{\phi 1}$ and $V_{\phi 2}$:

$$V_{\phi 1} = V_1^0 + \frac{V^E}{x_1} \quad (19)$$

$$V_{\phi 2} = V_2^0 + \frac{V^E}{x_2} \quad (20)$$

The apparent molar volumes, $V_{\phi i}$, are summarized in Table 3. The apparent and partial molar volumes of glycerol increase at all temperatures as the composition of glycerol in the mixture increases, in contrast to the apparent and partial molar volumes of butanediols which tend to decrease with the composition of glycerol and the rise of temperature. This means that the butanediols take up less volume in the mixture than in the pure component. The behavior of the partial molar volumes and the apparent molar volumes shows a reduction in the total volume of the compositions compared with simple linear additions. The decrease of the volume could be assigned to the strong hydrogen bonding that occurring from the dipole-dipole interactions between the butanediols and glycerol [27].

Thermal expansivities, α , were calculated from the density and V^E results, to allow better understanding of change in the solution structure during blending. Thermal expansion coefficients for pure components and compositions, respectively are expressed by Eqs. 21, 22:

$$\alpha_i = \frac{1}{V_i^0} \left(\frac{\partial V_i^0}{\partial T} \right)_P \quad (21)$$

$$\alpha = \frac{1}{V} \left[\left(\frac{\partial V^E}{\partial T} \right)_{P,x} + \sum_{i=1}^2 \alpha_i x_i V_i^0 \right] \quad (22)$$

Excess thermal expansibilities, α^E , were calculated using Eq. 23:

$$\alpha^E = \alpha - \sum_{i=1}^2 \Phi_i \alpha_i \quad (23)$$

where Φ_i is the volume fraction of the pure component i , defined as Eq. 24:

$$\Phi_i = \frac{x_i V_i^0}{\sum_{i=1}^2 x_i V_i^0} \quad (24)$$

The values of the thermal expansibilities α , and those of excess thermal expansivity, α^E , at various temperatures, are reported in Table 3. The coefficients of thermal expansion α for all the binary systems increase both with increasing x_1 concentration and temperature. Whereas the values of excess thermal expansion coefficients α^E are negative for the three mixtures of glycerol with 1,2-butanediol, with 1,3-butanediol and with 2,3-butanediol but positive in the case of the mixture with isomer 1,4-butanediol.

4.2 Optical properties

Values of refractive indices, n_D , and the refractive indices deviations at all the temperatures are given in Table 5 along with glycerol mole fraction, x_1 . Figure 2a–d shows that the Δn_D values are positive for all compositions and at all studied temperatures for all the mixtures where the magnitude of Δn_D increase with increasing temperature except for the mixture with 1,3-butanediol where negative values are noted and the magnitude decreases as temperature increases. The negative values of the excess refractive indices indicate the presence of specific molecular interactions between the components of the mixture, leading to changes in the polarization of light. This is in contrast to what might be expected on the basis of the refractive indices of the individual components of the mixture alone. It is also possible that the nanoscale structure of the mixture is complex, resulting in local variations in density affecting the behavior of light. Negative excess refractive indices are an interesting phenomenon that can be studied in detail using advanced experimental techniques and complex theoretical models. The curves $\Delta n_D = f(x_1)$ are slightly asymmetrical with maximums estimated to $\Delta n_{D,max} \cdot 10^{-2} = (0.183, 0.205, 0.223, 0.269, 0.319, 0.358)$ at $x_1 = 0.4063$ for the mixture with 1,2-butanediol, $\Delta n_{D,max} \cdot 10^{-2} = (0.307, 0.347, 0.402, 0.452, 0.492, 0.522)$ at $x_1 = 0.3994$ for the mixture with 1,4-butanediol, $\Delta n_{D,max} \cdot 10^{-2} = (0.153, 0.191, 0.216, 0.241, 0.266, 0.291)$ at $x_1 = 0.5022$ for the mixture with 2,3-butanediol and with minimums situated at $x_1 = 0.5002$ as

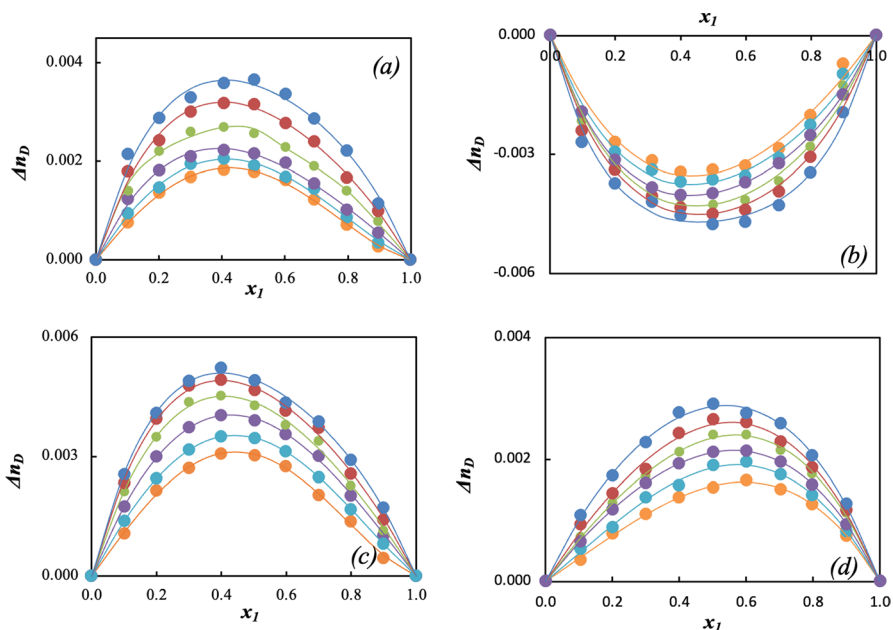


Fig. 2 Refractive index deviations vs mole fractions of glycerol for the glycerol (1) + butanediol isomer (2) mixtures at $T = [298.15\text{--}318.15]\text{ K}$ and atmospheric pressure: (a) glycerol (1) + 1,2-butanediol (2) mixture, (b) glycerol (1) + 1,3-butanediol (2) mixture, (c) glycerol (1) + 1,4-butanediol (2) mixture, (d) glycerol (1) + 2,3-butanediol (2) mixture. Circles: experimental data obtained in this work. Colors: (orange) 293.15 K, (sky blue) 298.15 K, (purple) 303.15 K, (green) 308.15 K, (red) 313.15, (blue) 318.15 K. Lines: represent the results obtained with RK polynomial (Color figure online)

$$\Delta n_{D,min} \cdot 10^{-2} = (-0.338, -0.363, -0.401, -0.425, -0.450, -0.476) \text{ for the mixture with 1,3-butanediol.}$$

4.3 Spectroscopic Properties

The spectroscopic IR has been used for the analysis of molecular interactions and the identification of the bonds present. The infrared spectra of each mixture have been recorded at room temperature at three glycerol compositions ($x_1 = 0.25$ or 0.5 and 0.75). Infrared spectra are presented in transmittance (fraction of the transmitted intensity with respect to the incident intensity) expressed in percentage and the abscissa axis as a function of the wave number (inverse of the wavelength), on axis directed to the left.

As shown by Fig. S1A–D, the IR spectra are relatively similar in the four mixtures for the same mole fraction of glycerol. The analysis reveals a (O–H) elongation band for pure 1,2-butanediol at (3326 cm^{-1}); for pure 1,3-butanediol at (3302 cm^{-1}), for pure 1,4-butanediol at (3294 cm^{-1}) and at (3348 cm^{-1}) for pure 2,3-butanediol typical of intermolecular OH functions. Increasing the concentration of glycerol

Table 5 Experimental refractive indices, n_D , and refractive index deviations, Δn_D , for the glycerol (1) + butanediol isomer (2) mixtures at temperatures (293.15 - 318.15) K and atmospheric pressure (101325 Pa)

x_1	n_D	$10^{-2}\Delta n_D$	n_D	$10^{-2}\Delta n_D$	n_D	$10^{-2}\Delta n_D$
Glycerol + 1,2-Butanediol						
293.15 K						
0.000	1.439	0.000	1.438	0.000	1.435	0.000
0.102	1.443	0.076	1.442	0.094	1.439	0.123
0.201	1.447	0.137	1.446	0.147	1.443	0.182
0.302	1.451	0.167	1.449	0.195	1.447	0.210
0.406	1.455	0.183	1.453	0.205	1.451	0.223
0.503	1.458	0.178	1.456	0.191	1.454	0.216
0.602	1.461	0.162	1.459	0.167	1.457	0.197
0.694	1.464	0.122	1.462	0.144	1.460	0.155
0.797	1.467	0.071	1.464	0.086	1.463	0.101
0.897	1.470	0.027	1.467	0.034	1.466	0.055
1.000	1.473	0.000	1.470	0.000	1.469	0.000
308.15 K						
0.000	1.433	0.000	1.432	0.000	1.430	0.000
0.102	1.438	0.154	1.437	0.179	1.436	0.213
0.201	1.442	0.217	1.441	0.242	1.440	0.287
0.302	1.446	0.250	1.445	0.300	1.444	0.330
0.406	1.450	0.269	1.449	0.319	1.448	0.358
0.503	1.453	0.266	1.452	0.316	1.452	0.365
0.602	1.456	0.227	1.455	0.277	1.455	0.336
0.694	1.459	0.190	1.458	0.240	1.458	0.286
0.797	1.462	0.141	1.461	0.166	1.461	0.222
0.897	1.464	0.075	1.464	0.100	1.463	0.115
1.000	1.467	0.000	1.466	0.000	1.466	0.000
Glycerol + 1,3-Butanediol						
293.15 K						
0.000	1.439	0.000	1.438	0.000	1.436	0.000
0.099	1.440	-0.192	1.439	-0.193	1.437	-0.225
0.200	1.443	-0.269	1.441	-0.294	1.440	-0.309
0.314	1.446	-0.316	1.445	-0.338	1.443	-0.361
0.401	1.449	-0.344	1.447	-0.369	1.445	-0.399
0.500	1.453	-0.338	1.450	-0.363	1.449	-0.401
0.598	1.456	-0.329	1.454	-0.355	1.452	-0.375
0.701	1.460	-0.285	1.457	-0.310	1.456	-0.337
0.799	1.464	-0.201	1.461	-0.226	1.460	-0.261
0.898	1.469	-0.072	1.466	-0.097	1.465	-0.115
1.000	1.473	0.000	1.470	0.000	1.469	0.000
308.15 K						
0.000	1.435	0.000	1.434	0.000	1.433	0.000
0.099	1.436	-0.215	1.435	-0.240	1.434	-0.270

Table 5 (continued)

x_1	n_D	$10^{-2}\Delta n_D$	n_D	$10^{-2}\Delta n_D$	n_D	$10^{-2}\Delta n_D$
0.200	1.438	-0.339	1.437	-0.339	1.436	-0.374
0.314	1.441	-0.380	1.440	-0.405	1.439	-0.420
0.401	1.444	-0.409	1.443	-0.434	1.442	-0.454
0.500	1.447	-0.425	1.446	-0.450	1.445	-0.476
0.598	1.450	-0.415	1.449	-0.440	1.448	-0.470
0.701	1.454	-0.367	1.453	-0.392	1.452	-0.427
0.799	1.458	-0.281	1.457	-0.306	1.456	-0.346
0.898	1.463	-0.125	1.461	-0.150	1.460	-0.195
1.000	1.467	0.000	1.466	0.000	1.466	0.000
Glycerol + 1,4-Butanediol						
	293.15 K		298.15 K		303.15 K	
0.000	1.439	0.000	1.438	0.000	1.437	0.000
0.100	1.444	0.107	1.443	0.129	1.442	0.174
0.200	1.448	0.214	1.447	0.259	1.446	0.299
0.301	1.452	0.270	1.451	0.313	1.450	0.373
0.399	1.456	0.307	1.454	0.347	1.454	0.402
0.503	1.459	0.302	1.458	0.340	1.457	0.390
0.599	1.462	0.275	1.460	0.310	1.460	0.355
0.700	1.465	0.204	1.463	0.261	1.462	0.301
0.800	1.468	0.137	1.465	0.166	1.465	0.201
0.899	1.470	0.045	1.468	0.072	1.467	0.102
1.000	1.473	0.000	1.470	0.000	1.469	0.000
	308.15 K		313.15 K		318.15 K	
0.000	1.436	0.000	1.435	0.000	1.434	0.000
0.100	1.441	0.212	1.440	0.234	1.439	0.254
0.200	1.446	0.349	1.445	0.394	1.444	0.409
0.301	1.450	0.435	1.449	0.478	1.448	0.488
0.399	1.453	0.452	1.452	0.492	1.452	0.522
0.503	1.456	0.428	1.455	0.466	1.455	0.490
0.599	1.458	0.380	1.458	0.415	1.457	0.435
0.700	1.461	0.338	1.460	0.371	1.460	0.386
0.800	1.463	0.226	1.462	0.256	1.462	0.291
0.899	1.465	0.114	1.464	0.142	1.464	0.172
1.000	1.467	0.000	1.466	0.000	1.466	0.000
Glycerol + 2,3-Butanediol						
	293.15 K		298.15 K		303.15 K	
0.000	1.431	0.000	1.430	0.000	1.428	0.000
0.104	1.436	0.036	1.434	0.054	1.433	0.068
0.200	1.440	0.078	1.439	0.088	1.437	0.118
0.299	1.445	0.110	1.443	0.138	1.442	0.158
0.400	1.449	0.137	1.447	0.157	1.446	0.192
0.502	1.454	0.153	1.452	0.191	1.451	0.216

Table 5 (continued)

x_1	n_D	$10^{-2}\Delta n_D$	n_D	$10^{-2}\Delta n_D$	n_D	$10^{-2}\Delta n_D$
0.600	1.458	0.166	1.456	0.196	1.455	0.211
0.704	1.462	0.152	1.460	0.175	1.459	0.194
0.799	1.466	0.126	1.463	0.141	1.462	0.161
0.900	1.470	0.075	1.467	0.082	1.466	0.092
1.000	1.473	0.000	1.470	0.000	1.469	0.000
	308.15 K		313.15 K		318.15 K	
0.000	1.426	0.000	1.425	0.000	1.423	0.000
0.104	1.431	0.074	1.430	0.093	1.429	0.108
0.200	1.436	0.128	1.434	0.143	1.433	0.173
0.299	1.440	0.173	1.439	0.183	1.438	0.228
0.400	1.445	0.212	1.444	0.242	1.443	0.277
0.502	1.449	0.241	1.448	0.266	1.447	0.291
0.600	1.453	0.241	1.452	0.261	1.451	0.276
0.704	1.457	0.214	1.456	0.229	1.456	0.259
0.799	1.461	0.176	1.460	0.186	1.459	0.207
0.900	1.464	0.112	1.463	0.117	1.463	0.127
1.000	1.467	0.000	1.466	0.000	1.466	0.000

Standard uncertainties: $u(x_1) = 0.002$, $u(n_D) = 0.004$, $u(T) = 0.03$ K

in the mixture leads to a shift of this band towards lower wavenumbers, reaching (3280 cm^{-1}) for pure glycerol. This shift could highlight the predominance of intermolecular interactions between 1,2-butanediol and glycerol in the dialcohol-rich region. Peak intensity increases with increasing glycerol composition.

4.4 Effect of Isomeric Position

The variation of volumetric properties of binary systems containing glycerol with butanediol isomers at $T = 298.15$ K follows the sequence: (Glycerol + 2,3-Butanediol) > (Glycerol + 1,2-Butanediol) > (Glycerol + 1,4-Butanediol) > (Glycerol + 1,3-Butanediol). However, an opposite sequence is observed for the absolute values of the refractive indices, which leads us to consider the impact of positional isomers: the closer the hydroxyl groups in the butanediol isomer, the stronger the intermolecular interactions with glycerol.

4.5 Modeling of Density and Refractive Index

In this study, we have used the experimental density data (obtained in this work) and the vapor pressure data from DIPPR [28] to calculate the fitted parameters of PC-SAFT EoS in the temperature range of 293.15 K to 318.15 K. The absolute

Table 6 The fitted parameters required in PC-SAFT EoS and the absolute average deviation in vapor pressure and liquid density

Fluid	m	σ (Å)	ϵ/k_B (K)	κ^{AB}	ϵ^{AB}/k_B (K)	%AADP	%AAD ρ
Glycerol	4.5000	2.9136	339.5548	0.0595	646.9368	0.13	0.25
1,2-Butanediol	4.0000	3.1733	216.3501	0.0877	1881.3562	0.02	0.01
1,3-Butanediol	3.7000	3.2802	264.6000	0.0580	1640.5211	0.00	0.05
1,4-Butanediol	3.7000	3.2767	263.0404	0.0504	2012.4788	0.01	0.07
2,3-Butanediol	4.1000	3.1749	266.0064	0.0914	961.4177	0.13	0.02
Overall						0.06	0.08

Table 7 Absolute average deviation for density and refractive indices using predictive approaches

Mixture	%AAD ρ	%AAD n_D
Glycerol + 1,2-Butanediol	0.37	0.05
Glycerol + 1,3-Butanediol	0.29	0.22
Glycerol + 1,4-Butanediol	0.24	0.21
Glycerol + 2,3-Butanediol	0.21	0.12
Overall	0.28	0.15

average deviation for property X and the objective function to obtain the fitted parameters required in PC-SAFT EoS are given Eqs. 25 and 26, respectively:

$$\%AADX = \frac{100}{N} \sum_{i=1}^N \frac{|X_i^{Exp.} - X_i^{Theo.}|}{X_i^{Exp.}} \quad (25)$$

$$OF(m, \sigma, \epsilon/k_B, \epsilon^{AB}/k_B, \kappa^{AB}) = \sum_{i=1}^N \left(\frac{P_i^{DIPPR} - P_i^{Theo.}}{P_i^{DIPPR}} \right)^2 + \left(\frac{\rho_i^{Exp.} - \rho_i^{Theo.}}{\rho_i^{Exp.}} \right)^2 \quad (26)$$

where P is the vapor pressure for pure fluid, $X = \rho, n_D$, and $Theo.$ is related to the theoretical value. The fitted parameters are published in Table 6. According to Table 6, PC-SAFT EoS correctly fit the compressed liquid density and the vapor pressure. The overall deviations are 0.06 % and 0.08 % for vapor pressure and liquid density, respectively.

On the other hand, in this work, we have used a predictive approach to calculate the density and refractive index of binary mixtures, i.e., using PC-SAFT EoS and Laplace mixing rule + PC-SAFT EoS, respectively. It is a great advantage of not requiring fitted parameters in binary mixtures. According to the Table 7, the overall deviation was 0.28 % and 0.15 % for density and refractive index. We have also used PC-SAFT to predict the experimental density data for glycerol + 2,3-butanediol mixture obtained by Alavianmehr et al [25]; the deviation was 0.80 %. Figures 3 and 4 show the behavior of the liquid density and refractive index for glycerol + 2,3-butanediol at different temperatures, respectively. According to Fig. 3, the liquid

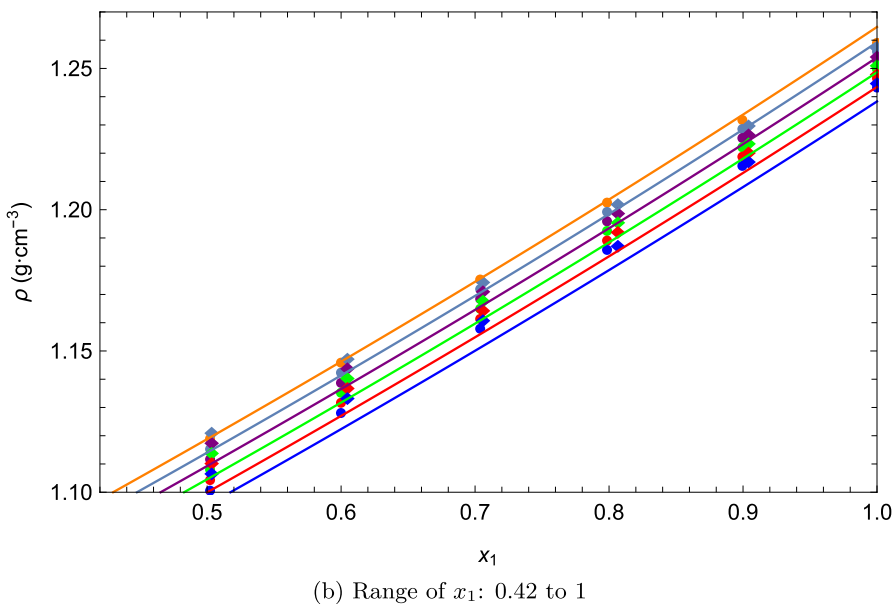
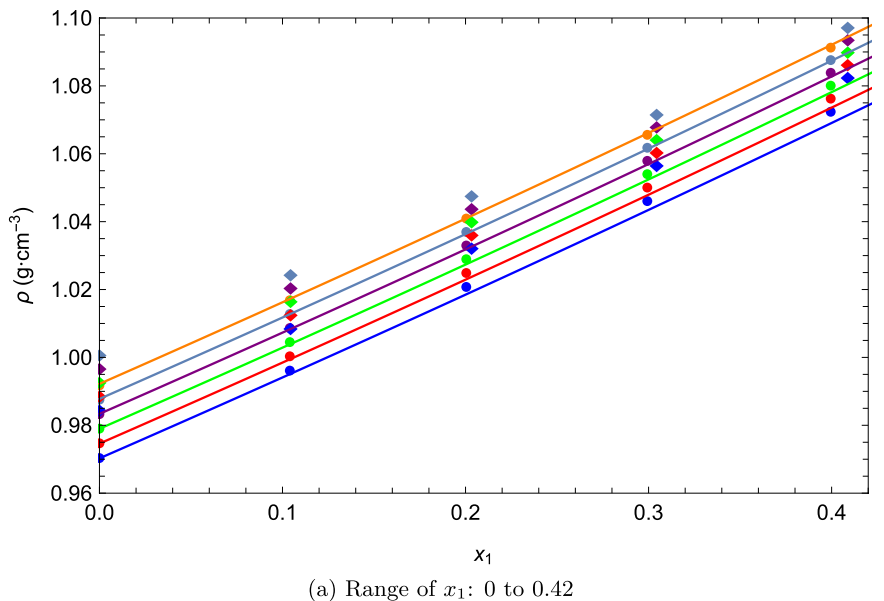


Fig. 3 Liquid densities for glycerol (1) + 2,3-butanediol (2) mixture at different temperatures. Circles: experimental data obtained in this work. Diamond: experimental data obtained from Alavianmehr et al [25]. Colors: (orange) 293.15 K, (sky blue) 298.15 K, (purple) 303.15 K, (green) 308.15 K, (red) 313.15, (blue) 318.15 K. Lines: represent the results obtained with PC-SAFT EoS (Color figure online)

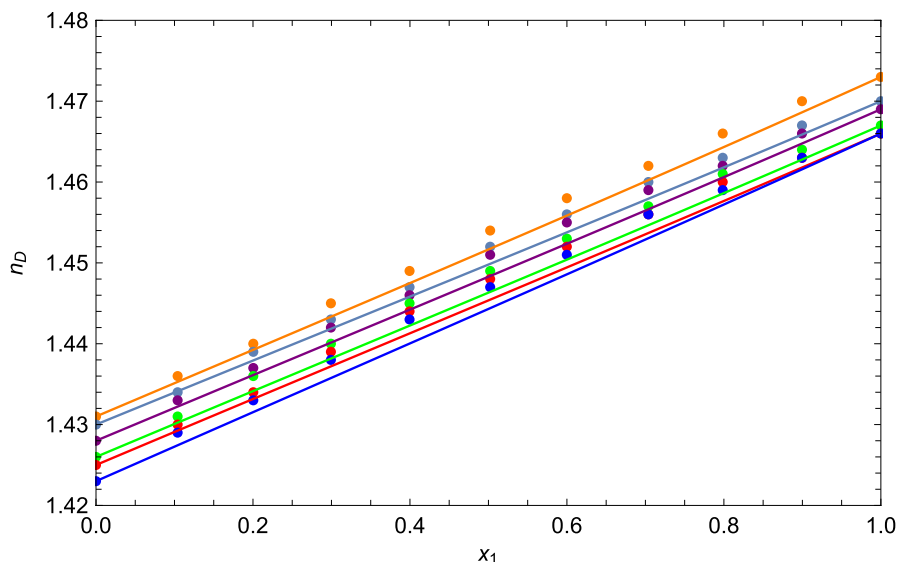


Fig. 4 Refractive indices for glycerol (1) + 2,3-butanediol (2) mixture at different temperatures. Circles: experimental data obtained in this work. Colors: (orange) 293.15 K, (sky blue) 298.15 K, (purple) 303.15 K, (green) 308.15 K, (red) 313.15, (blue) 318.15 K. Lines: represent the results obtained with PC-SAFT EoS + Laplace mixing rule (Color figure online)

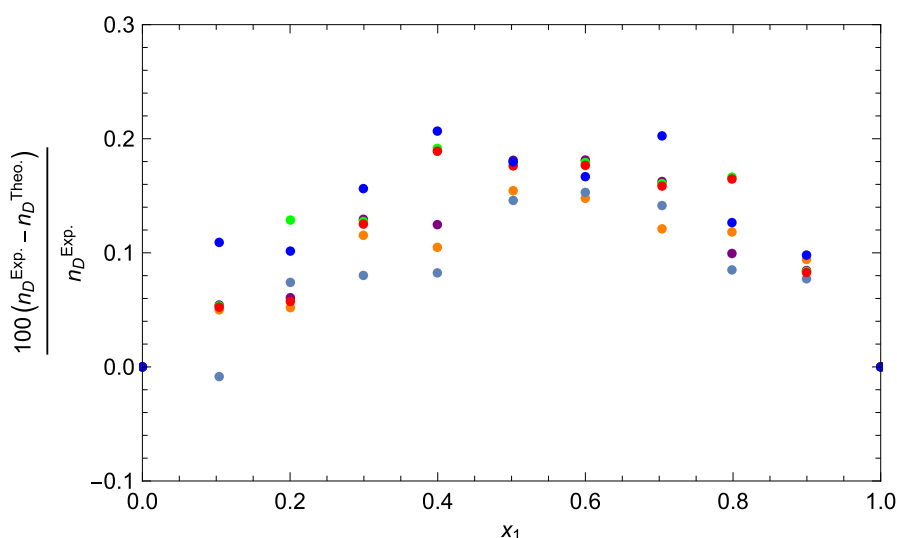


Fig. 5 Percentage deviation for refractive index at each composition and temperature for glycerol (1) + 2,3-butanediol (2) mixture at different temperatures. Circles: values of the percentage deviations. Colors: (orange) 293.15 K, (sky blue) 298.15 K, (purple) 303.15 K, (green) 308.15 K, (red) 313.15, (blue) 318.15 K (Color figure online)

density obtained by us and Alavianmehr et al [25] is well predicted by PC-SAFT EoS. From the Fig. 4, it is observed that PC-SAFT EoS + Laplace mixing rule underpredicts the refractive index for a part of the glycerol mole fraction range and depending on temperature. Fig. 5 shows a graph of deviations of the refractive index for the glycerol + 2,3-butanediol mixture at different compositions and temperatures. The deviations are between approximately 0 and 0.2 %. Furthermore, it is consistent that in mole fractions 0 and 1, the deviations are 0 %, because PC-SAFT + Laplace mixing rule is not capable of predicting the refractive index of pure fluids.

5 Conclusions

In this work, some thermophysical properties (density and refractive index) covered the whole composition range of glycerol + butanediol isomer have been measured at several temperatures between 293.15 K to 318.15 K and atmospheric pressure. Some derivatives have been calculated such as excess molar volumes, partial molar volumes, apparent molar volumes, thermal isobaric expansibilities, excess thermal expansibilities, partial molar volumes at infinite dilution. The results suggest the presence of strong interactions between unlike molecules across intermolecular hydrogen bonding confirmed by spectroscopic infrared measurements. The thermophysical properties of the studied mixtures show that changes in temperature, in composition in structure and in the position of hydroxyl groups have a significant influence on the molecular environment. Liquid density of binary mixtures was correctly predicted with PC-SAFT EoS (overall deviation = 0.28 %). Furthermore, the deviation in refractive index obtained with Laplace's rule is low (overall deviation = 0.15%).

Supplementary Information The online version contains supplementary material available at <https://doi.org/10.1007/s10765-023-03272-5>.

Acknowledgments A.H acknowledges the economic support given by the UCSC.

Author Contributions YC: Experimental investigation, Writing. AH: Theoretical investigation, Writing. FA: Experimental investigation, Writing.

Funding The authors have not disclosed any funding.

Data Availability All data generated or analyzed during this study are included in this article and its supplementary information files.

Declarations

Conflict of interest The authors have not disclosed any competing interests.

References

1. P.C. Shukla, G. Belgiorno, G. Di Blasio, A.K. Agarwal, *Alcohol as an alternative fuel for internal combustion engines* (Springer, Singapore, 2021)

2. A. Basile, F. Dalena, *Alcohols and bioalcohols: characteristics, production, and uses* (Nova Science Publishers, Inc., New York, 2015)
3. M. Pagliaro, M. Rossi, *The future of glycerol* (Royal Society of Chemistry, Cambridge, 2010)
4. C.J. Mota, B.P. Pinto, A.L. de Lima, *Glycerol: a versatile renewable feedstock for the chemical industry* (Springer, Cham, 2017)
5. A. Mustain, E.D. Setiawati, R. Tetrisyanda, G. Wibawa, Experimental and predicted values of bubble point pressure for binary and ternary systems consisting of 1-butanol, 2-methyl-1-propanol, glycerol, and water. *J. Chem. Eng. Data* **67**, 941–947 (2022)
6. V.B. Vicente, G.V. Olivieri, R.G. dos Santos, R.B. Torres, Volumetric properties of binary mixtures of glycerol+ alkanols (c1–c4): Experimental study and application of the peng–robinson–stryjek–vera equation of state. *J. Chem. Thermodyn.* **168**, 106728 (2022)
7. M. Tyczyńska, A. Dentkiewicz, M. Jóźwiak, Thermodynamic and thermal analyze of n, n-dimethyl-formamide+ 1-butanol mixture properties based on density, sound velocity and heat capacity data. *Molecules* **28**, 4698 (2023)
8. E.V. Anslyn, D.A. Dougherty, *Modern physical organic chemistry* (University science books, Sausalito, 2005)
9. G.I. Egorov, D.M. Makarov, Volumetric properties of binary mixtures of glycerol + tert-butanol over the temperature range 293.15 to 348.15 k at atmospheric pressure. *J. Solut. Chem.* **41**, 536–554 (2012)
10. M.-L. Ge, J.-L. Ma, B. Chu, Densities and viscosities of propane-1, 2, 3-triol + ethane-1, 2-diol at $T=(298.15 \text{ to } 338.15) \text{ k}$. *J. Chem. Eng. Data* **55**, 2649–2651 (2010)
11. B. Hawrylak, K. Gracie, R. Palepu, Thermodynamic properties of binary mixtures of butanediols with water. *J. Solut. Chem.* **27**, 17–31 (1998)
12. Q.-S. Li, Y.-M. Tian, S. Wang, Densities and excess molar volumes for binary mixtures of 1, 4-butanediol+ 1, 2-propanediol,+ 1, 3-propanediol, and+ ethane-1, 2-diol from (293.15 to 328.15) k. *J. Chem. Eng. Data* **53**, 271–274 (2008)
13. Y. Matsumoto, H. Touhara, K. Nakanishi, N. Watanabe, Molar excess enthalpies for water+ ethanediol,+ 1, 2-propanediol, and+ 1, 3-propanediol at 298.15 k. *J. Chem. Thermodyn.* **9**, 801–805 (1977)
14. Anton Paar GmbH, Digital densimeter: *Instuction manual DMA 5000*, (2009)
15. K.R. Hall, D.J. Kirwan, O.L. Updike, Reporting precision of experiments. *Chem. Eng. Educ.* **9**, 24–30 (1975)
16. J. Gross, G. Sadowski, Perturbed-chain saft: an equation of state based on a perturbation theory for chain molecules. *Ind. Eng. Chem. Res.* **40**, 1244–1260 (2001)
17. J. Gross, G. Sadowski, Application of the perturbed-chain saft equation of state to associating systems. *Ind. Eng. Chem. Res.* **41**, 5510–5515 (2002)
18. M. Almasi, A. Hernández, Experimental and theoretical studies of ethylene glycol dimethyl ether and 2-alkanol mixtures. *Int. J. Thermophys.* **44**, 109 (2023)
19. A. Hernández, A.Z. Zeqiraj, F.R. Aliaj, Densities, sound speeds, and refractive indices of 1-propanol+ cyclohexane (or cyclohexene or cyclohexanone) binary mixtures at various temperatures under atmospheric pressure: experimental and modeling study. *Int. J. Thermophys.* **44**, 102 (2023)
20. R. Abidi, M. Hichri, C. Lafuente, A. Hernández, Surface tensions for binary mixtures of alkyl levulinate+ alkanol: measurement and modeling. *Int. J. Thermophys.* **44**, 33 (2023)
21. B. Giner, C. Lafuente, A. Villares, M. Haro, M.C. Lopez, Volumetric and refractive properties of binary mixtures containing 1, 4-dioxane and chloroalkanes. *J. Chem. Thermodyn.* **39**, 148–157 (2007)
22. N.L. Benkelfat-Seladji, F. Ouaar, A. Hernández, N. Muñoz-Rujas, I. Bahadur, N.C.-B. Ahmed, E. Montero, L. Negadi, Measurements and modeling of physicochemical properties of pure and binary mixtures containing 1, 2-dimethoxyethane and some alcohols. *J. Chem. Eng. Data* **66**, 3397–3416 (2021)
23. N.L. Benkelfat-Seladji, F. Ouaar, A. Hernández, I. Bahadur, N. Muñoz-Rujas, S.K. Singh, E. Montero, N.C.-B. Ahmed, L. Negadi, Density, speed of sound, refractive index of binary mixtures containing 2-ethoxyethanol and some alcohols: measurement and correlation. *J. Chem. Thermodyn.* **66**, 106762 (2022)
24. O. Redlich, A.T. Kister, Algebraic representation of thermodynamic properties and the classification of solutions. *Ind. Eng. Chem.* **40**, 345–348 (1948)

25. M.M. Alavianmehr, R. Ahmadi, N. Aguilar, M. El-Shaikh, S.M. Hosseini, S. Aparicio, Thermo-physical and molecular modelling insights into glycerol+ alcohol liquid mixtures. *J. Mol. Liq.* **297**, 111811 (2020)
26. H. Iloukhani, M. Almasi, Densities, viscosities, excess molar volumes, and refractive indices of acetonitrile and 2-alkanols binary mixtures at different temperatures: experimental results and application of the prigogine-flory-patterson theory. *Thermochim. Acta* **495**, 139–148 (2009)
27. A.S. Alkindi, Y.M. Al-Wahaibi, A.H. Muggeridge, Physical properties (density, excess molar volume, viscosity, surface tension, and refractive index) of ethanol+ glycerol. *J. Chem. Eng. Data* **53**, 2793–2796 (2008)
28. T.E. Daubert, R.P. Danner, *Physical and thermodynamic properties of pure chemicals data compilation* (Taylor & Francis, Bristol, 2004)

Publisher's Note Springer Nature remains neutral with regard to jurisdictional claims in published maps and institutional affiliations.

Springer Nature or its licensor (e.g. a society or other partner) holds exclusive rights to this article under a publishing agreement with the author(s) or other rightsholder(s); author self-archiving of the accepted manuscript version of this article is solely governed by the terms of such publishing agreement and applicable law.

Authors and Affiliations

Yasmine Chabouni¹ · Ariel Hernández² · Fouzia Amireche¹

 Ariel Hernández
ahernandez@ucsc.cl

¹ Crystallography and Thermodynamics Laboratory, Faculty of Chemistry, University of Sciences and Technology HouariBoumediene, PO Box 32 El Alia, 16111 Bab Ezzouar, Algiers, Algeria

² Departamento de Ingeniería Industrial, Facultad de Ingeniería, Universidad Católica de la Santísima Concepción, Alonso de Ribera, 2850 Concepción, Chile